A Low Complexity Subband Adaptive Equaliser for Broadband MIMO Channels

Viktor Bale and Stephan Weiss
Communications Research Group, School of Electronics & Computer Science
University of Southampton, Southampton SO17 1BJ, UK
{vb01r,sw1}@ecs.soton.ac.uk

ABSTRACT

This paper addresses trained adaptation of broadband multiple-input multiple-output (MIMO) equalisers operating in severely time-dispersive environments which result in slow convergence and poor performance for least mean squares (LMS) type algorithms. We present a subband approach, which enhances a normalised LMS (NLMS) convergence by prewhitening of the input signals and reduces its computational complexity. Equalisation based on the recursive least squares (RLS) algorithm in the time domain is prohibitive due to its high complexity, which can be drastically reduced by the subband approach to an extend such that the overall RLS cost for convergence may be much lower than the subband NLMS. The performance of the various systems is compared in simulations.

1 INTRODUCTION

To exploit substantial capacity improvements offered by broadband multiple-input multiple-output (MIMO) transmission channels [1], the time-dispersiveness and cross-coupling of the MIMO channel has to be mitigated, often requiring equalisers of high computational complexity in the receiver. If high data rate wireless links are envisaged, the resulting severe dispersiveness poses a considerable challenge in terms of the number of parameters, the convergence speed, and the real-time implementation of an adaptive equaliser.

Long impulse responses can also be found in acoustic systems, where containment of the computational complexity has motivated frequency domain methods in [2, 3] to solve the problem of multichannel deconvolution off-line, where the MMSE time-domain process would impose too great a computational load [4]. Adaptive frequency domain methods satisfying broadband optimality are addressed in [5, 6]. Subband methods utilising filter banks of higher selectivity than the DFT can be employed to create subband signals, which can be processed independently. Such subband methods have been successfully applied to acoustic MIMO channel deconvolution in [7, 8] yielding substantial improvements in computational complexity and additionally increased convergence speed for LMS-type algorithms. In this paper, we consider the approach in [8] for MIMO communications channels, and additionally examine the use of reduced complexity recursive least squares algorithms in the subband domain.

Sec. 2 outlines the MIMO system model used in this paper and states the MMSE MIMO linear equaliser. The later will be used to benchmark adaptive MIMO equalisers in Sec. 3 and subband adaptive realisations in Sec. 4. In order to compare the performance of the algorithms, simulations are presented in Sec. 5.

2 SYSTEM MODEL AND ANALYTIC INVERSION

2.1 MIMO Channel and Assumptions

The P receiver outputs of a MIMO channel excited by M transmitters can be written as

$$\mathbf{y}[n] = \mathbf{H}\mathbf{x}[n] + \mathbf{v}[n] \tag{1}$$

where $\mathbf{y}[n] \in \mathbb{C}^{PL_w}$ contains P stacked vectors of the received signals,

$$\mathbf{y}[n] = \begin{bmatrix}\mathbf{y}_1^{\mathrm{T}}[n] & \mathbf{y}_2^{\mathrm{T}}[n] & \cdots \mathbf{y}_P^{\mathrm{T}}[n]\end{bmatrix} \tag{2}$$

with $\mathbf{y}_p[n]$, $p = 1, 2, \cdots P$, holding L_w tap delay line values of the pth received signal at time n. The vector $\mathbf{v}[n] \in \mathbb{C}^{PL_w}$ comprises of channel noise samples corrupting the P received signals, organised in vectorial form analogously to (2), whereby the variable L_g reflects the length of an equaliser. Further in (1), $\mathbf{x} \in \mathbb{C}^{M(L_w+L_h-1)}$ holds the M stacked vectors of the transmitted signal, such that each transmitter contributes a window of $L_w + L_h - 1$ samples to $\mathbf{x}[n]$, where L_h is the length of each sub-channel comprising the MIMO system. Finally, the MIMO system is given in form of the matrix $\mathbf{H}$ [4]

$$\mathbf{H} = \begin{bmatrix} \mathbf{H}_{11} & \mathbf{H}_{21} & \cdots & \mathbf{H}_{M1} \\ \mathbf{H}_{12} & \mathbf{H}_{22} & \cdots & \mathbf{H}_{M2} \\ \vdots & \vdots & \ddots & \vdots \\ \mathbf{H}_{1P} & \mathbf{H}_{2P} & \cdots & \mathbf{H}_{MP} \end{bmatrix} \tag{3}$$

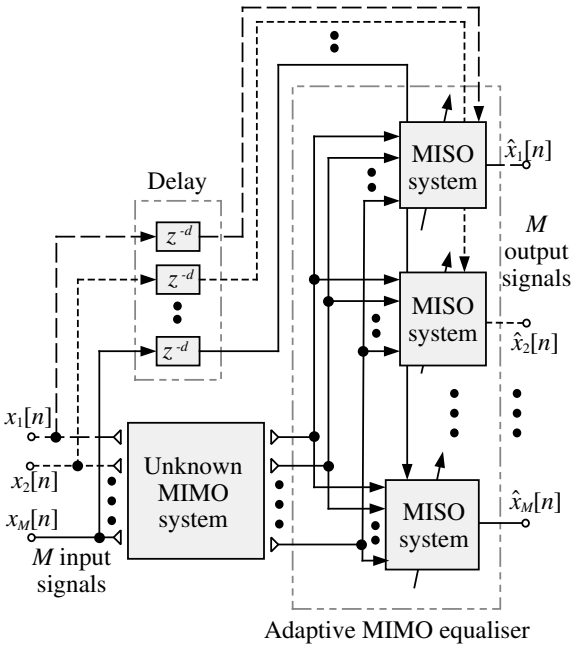

Figure 1: Block diagram showing adaptive system set-up to obtain the response for the inverse of an unknown system.

where the submatrices $\mathbf{H}_{mp} \in \mathbb{C}^{L_w \times L_w + L_h - 1}$,

$$\mathbf{H}_{mp}^{\mathrm{T}} = \begin{bmatrix} h_{mp}[0] & 0 & \cdots & \mathbf{0} \\ h_{mp}[1] & h_{mp}[0] & \ddots & \vdots \\ \vdots & h_{mp}[1] & \ddots & 0 \\ h_{mp}[L_h-1] & \vdots & \ddots & h_{mp}[0] \\ 0 & h_{mp}[L_h-1] & \ddots & h_{mp}[1] \\ \vdots & \ddots & \ddots & \vdots \\ 0 & \cdots & 0 & h_{mp}[L_h-1] \end{bmatrix} , \quad (4)$$

represent convolutional matrices comprising of the channel impulse response (CIR) coefficients $h_{mp}[n]$ between the pth transmitter and the mth receiver, with $\{\cdot\}^{\mathrm{T}}$ denoting transposition.

We assume that the input signals $x_m[n]$ are independent of the additive channel noise $\mathbf{v}[n]$. Both $x_m[n]$, $m = 1, 2, \cdots M$, and $\mathbf{v}[n]$ are further zero mean with covariance matrices $\mathbf{R}_{xx} = \mathcal{E}\{\mathbf{x}[n]\mathbf{x}^{\mathrm{H}}[n]\}$, $\mathbf{R}_{vv} = \mathcal{E}\{\mathbf{v}[n]\mathbf{v}^{\mathrm{H}}[n]\}$, and $\mathbf{R}_{xv} = \mathcal{E}\{\mathbf{x}[n]\mathbf{v}^{\mathrm{H}}[n]\} = \mathbf{0} \in \mathbb{Z}^{M(L_w+L_h-1)\times PL_w}$, where $\mathcal{E}\{\cdot\}$ is the expectation operator.

2.2 MMSE MIMO Equaliser

We consider linear MIMO equalisation, for which the setup is shown in Fig. 1, employing a multiple input single output (MISO) system with P inputs to recover each of the M transmitted signals. This MISO system is further characterised in Fig. 2, where filters with impulse responses $w_{mp}[n]$ process the pth received signal in the

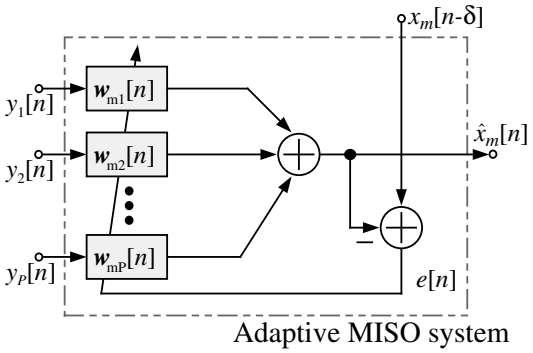

Figure 2: A basic MISO adaptive system.

mth MISO system. We can stack the responses of the mth MISO system and define

$$\mathbf{w}_m = [\mathbf{w}_{m1}^{\mathrm{T}} \; \mathbf{w}_{m2}^{\mathrm{T}} \; \cdots \; \mathbf{w}_{mP}^{\mathrm{T}}]^{\mathrm{H}} \quad (5)$$

whereby

$$\mathbf{w}_{mp} = [w_{mp}[0] \; w_{mp}[1] \; \cdots \; w_{mp}[L_w - 1]]^{\mathrm{T}} \quad . \quad (6)$$

Thus the mth MIMO system output $\hat{x}_m[n]$ is given by

$$\hat{x}_m[n] = \mathbf{w}_m^{\mathrm{H}} \mathbf{y}[n] \quad . \quad (7)$$

With a suitable pinning vector $\mathbf{d}_m$ extracting a delayed sample of the mth transmitted signal from the input vector $\mathbf{x}[n]$ in (1), we can formulate the MMSE problem for the mth MISO equaliser as

$$\mathbf{w}_{m,\mathrm{MMSE}} = \arg\min_{\mathbf{w}_m} \mathcal{E}\{|\hat{x}_m[n] - \mathbf{d}_m^{\mathrm{H}}\mathbf{x}[n]|^2\} \quad . \quad (8)$$

By expanding the MMSE cost function,

$$\begin{aligned} \xi &= \mathcal{E}\{|\hat{x}_m[n] - \mathbf{d}_m^{\mathrm{H}}\mathbf{x}[n]|^2\} & (9) \\ &= \mathbf{w}_m^{\mathrm{H}}\mathbf{H}\mathbf{R}_{xx}\mathbf{H}^{\mathrm{H}}\mathbf{w}_m + \mathbf{w}_m^{\mathrm{H}}\mathbf{R}_{vv}\mathbf{w}_m - \mathbf{w}_m^{\mathrm{H}}\mathbf{H}\mathbf{R}_{xx}\mathbf{d}_m - \\ &\quad \mathbf{d}_m^{\mathrm{H}}\mathbf{R}_{xx}\mathbf{H}^{\mathrm{H}}\mathbf{w}_m + \mathbf{d}_m^{\mathrm{H}}\mathbf{R}_{xx}\mathbf{d}_m \quad , & (10) \end{aligned}$$

the Wiener solution is obtained via

$$\frac{\partial \xi}{\partial \mathbf{w}_m^*} = (\mathbf{H}\mathbf{R}_{xx}\mathbf{H}^{\mathrm{H}} + \mathbf{R}_{vv})\mathbf{w}_m - \mathbf{H}\mathbf{R}_{xx}\mathbf{d}_m \;=\; 0 \quad (11)$$

as

$$\mathbf{w}_{m,\mathrm{MMSE}} = (\mathbf{H}\mathbf{R}_{xx}\mathbf{H}^{\mathrm{H}} + \mathbf{R}_{vv})^{-1}\mathbf{H}\mathbf{R}_{xx}\mathbf{d}_m \quad (12)$$

for the mth MISO system. Therefore, by stacking

$$\mathbf{W} = [\mathbf{w}_1 \; \mathbf{w}_2 \; \cdots \; \mathbf{w}_M] \quad \in \mathbb{C}^{PL_w \times M} \quad (13)$$

and

$$\mathbf{D} = [\mathbf{d}_1 \; \mathbf{d}_2 \; \cdots \; \mathbf{d}_M] \quad \in \mathbb{Z}^{M(L_w+L_h-1)\times M} \quad (14)$$

we obtain the MIMO Wiener solution as

$$\mathbf{W}_{\mathrm{MMSE}} = \left(\mathbf{H}\mathbf{R}_{xx}\mathbf{H}^{\mathrm{H}} + \mathbf{R}_{vv}\right)^{-1}\mathbf{H}\mathbf{R}_{xx}\mathbf{D} \quad . \quad (15)$$

The MMSE solution provided by (15) can be numerically unstable if the inversion term is ill-conditioned, although the channel noise contributes a regularisation. Further, the high computational complexity of order $\mathcal{O}\{(M(L_w + L_h))^3\}$ in terms of multiply accumulates (MACs) is prohibitive, and non-stationarities in the MIMO channel may require to frequently re-calculate $\mathbf{W}_{\mathrm{MMSE}}$. Hence, in the following sections we will explore adaptive methods to estimate $\mathbf{W}_{\mathrm{MMSE}}$.

3 ADAPTIVE MIMO EQUALISATION

An adaptive solution to equalise a MIMO channel can be based on the system configuration shown in Fig. 1, whereby the problem is separated into M independent MISO systems, which can be characterised by the block diagram shown in Fig. 2. The later can be solved by any standard multichannel adaptive algorithm, whereby the filter responses $\mathbf{w}_{mp}$ in Fig. 2 are as defined in (6), but are associated with a time index n to account for the potential modification of coefficients over time.

If the P channels of the mth MISO multichannel adaptive filter are stacked according to (5), and the TDL vectors $\mathbf{y}[n]$ are organised as in (2), then the least mean square (LMS) algorithm is given by

$$\mathbf{w}_m[n+1] = \mathbf{w}_m[n] + \mu\, e_m^*[n]\mathbf{y}[n] \quad , \tag{16}$$

where the error $e_m[n]$ is calculated between the MISO output and a delayed version of the mth transmitted signal. A normalised LMS (NLMS) can be operated by defining

$$\mu = \tilde{\mu}/(\mathbf{y}^H[n]\mathbf{y}[n] + \alpha) \tag{17}$$

with $0 < \tilde{\mu} < 2$ and a small constant α to avoid division by zero.

We assume complex baseband data and filter coefficient, such that the computational cost of the NLMS accrues to

$$C_{\mathrm{fb,NLMS}} = M(8PL_w + 8P) \tag{18}$$

real valued MACs, whereby a complex valued MAC requires the calculation of 4 real valued ones.

The convergence of the NLMS defined by (16) and (17) is governed by the eigenvalue spread of $\mathbf{R}_{yy} = \mathcal{E}\{\mathbf{y}^{\mathrm{H}}[n]\mathbf{y}[n]\}$, which in turn depends on the frequency selectivity of the MIMO channel in $\mathbf{H}$ and the correlation between the P received signals $y_p[n]$ [19]. Hence, potentially due to high frequency selectivity and inter-channel correlations, slow convergence of LMS-type adaptive algorithms is anticipated.

It is well-known that a recursive least squares (RLS) algorithm is insensitive to the eigenvalue spread, but its use is impeded by a prohibitively large computation cost of

$$C_{\mathrm{fb,RLS}} = M(12(PL_w)^2 + 12(PL_w)) \tag{19}$$

MACs per fullband sampling period [19].

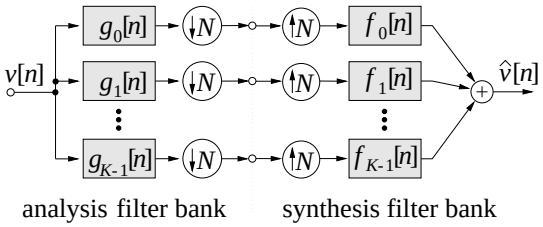

Figure 3: Subband decomposition by mean of analysis and synthesis filter banks.

In order to overcome both slow convergence and reduce the complexity of an adaptive algorithm, we consider subband solutions in the following section.

4 SUBBAND SOLUTION

4.1 Subband Decomposition and Processing

Subband based methods rely on analysis filter banks as shown in Fig. 3 to split a fullband signal into several frequency bands by a series of K filters $f_k[n]$, $k = 0, 1, \cdots K-1$. Due to their reduced bandwidth, the filter outputs can be decimated by a factor $N \leq K$. From these subband signals, a fullband signal can be restored by upsampling and interpolation filtering with a set of suitable synthesis filters $g_k[n]$, whereby the combined system of expanders and filters is referred to as synthesis filter bank.

Advantages over executing operations in the fullband arise because (i) processing in the subband domain occurs at an N times lower update rate, (ii) filters can be approximately N times shorter, (iii) the subband processors can be operated independent of each other, and (iv) the division into spectral intervals pre-whitens the subband signals [20, 18].

However, for critical decimation, $N = K$, spectral aliasing limits the performance of any processing in the subband domain, which can be mitigated by taking inter-subband correlations explicitly into accounts when designing subband based algorithms [18]. A simpler approach is to oversample subbands, i.e. decimate by a factor of $N < K$ [20], which can efficiently suppress aliasing in subbands and permits subbands to be processed independently.

4.2 Oversampled Modulated Filter Banks

Oversampled subbands with $N < K$ can be produced by oversampled filter banks, which are conveniently based on the modulation of a prototype lowpass filter common to both the analysis and synthesis stage. An example for a filter bank with $K = 16$ channels and decimation by $N = 14$ is shown in Fig. 4, whereby only the first 8 filter magnitude responses $F_k(e^{j\Omega}) \bullet\!\!-\!\!\circ\, f_k[n]$ are given.

Using polyphase analysis, the analysis filter bank can be separated into filtering operations with sections of

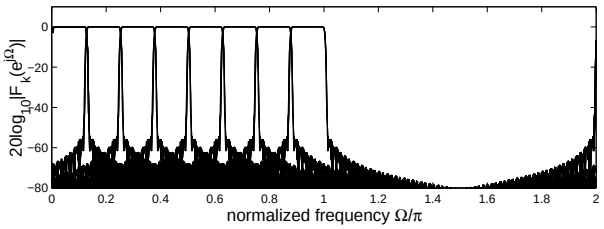

Figure 4: Filter bank characteristic for $K = 16$ and $N = 14$ based on a prototype with $L_p = 448$ coefficients.

the prototype filter followed by the modulating transform [13, 14], for which we have used a generalised discrete Fourier transform [17]. A modulated filter bank therefore offers advantages in terms of memory use, since only the prototype coefficients need to be stored, and computational complexity, which accrues to [14]

$$C_{\text{bank}} = (2L_p + 4K\log_2 K + 8K)/N \qquad (20)$$

for each analysis or synthesis filter bank per fullband sampling period, whereby L_p is the length of the prototype filter.

4.3 MIMO Equalisation in Subbands

The general approach to subband MIMO equalisation is given in Fig. 5. We apply an analysis filter bank operation to each of the P received signals, in order to operate the M MISO equalisers in the subband domain. To accomplish this, the M transmitted signals also need to be decomposed to form desired signals in the subband domain. If the signals are decomposed into K frequency bands, then each of the M MISO fullband systems is replaced by K independently operating MISO subband blocks.

Finally, each of the M equalised output signal can be obtained from reconstructing the K subband MISO equaliser outputs for each subsystem as shown in Fig. 5 by a synthesis filter bank. Hence, our proposed subband MIMO equaliser structure requires the calculation on $P + M$ analysis and M synthesis filter banks, as well as MK subband MISO adaptive filters. Each of the MISO subband blocks draws P inputs, which are sampled at an N times lower rate than the fullband algorithm. Further, due to extended sampling period, in order to achieve a similar modelling capability than a fullband MISO equaliser, the filter length can be shortened by an approximate factor of N. For the later, we neglect the conservative rule that due to fractional sampling the subband filters should be longer than L_w/N by an amount proportional to the prototype length L_p of the filter banks [18].

Using an NLMS algorithm in conjunction with the proposed subband MIMO equalisation structure, the computational cost incurred is given by

$$C_{\text{sb,NLMS}} = \frac{KM}{N}(8P\frac{L_w}{N} + 8P) +$$

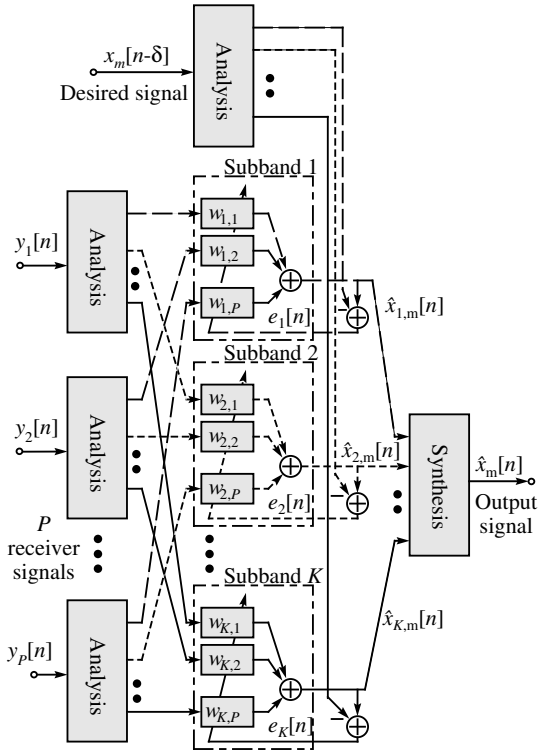

Figure 5: A MISO subband adaptive filter.

$$+ \ (P + 2M)C_{\text{bank}} \quad . \qquad (21)$$

If the temporal dimension L_w is sufficiently large, as required for a severally time-dispersive channel, then the filter bank contribution to (21) can be neglected. As a result, the complexity is reduced by a factor of N compared to (18), provided that a very moderate oversampling ratio $K/N \approx 1$ is employed. Further, the NLMS benefits from the temporal prewhitening arising from the subband decomposition, although spatial correlation between the P received signals processed by each of the KM MISO subband equalisers may still inhibit convergence.

Looking at the adaptation of the subband MISO equalisers using the RLS algorithm, we can note its complexity as

$$C_{\text{sb,RLS}} = \frac{KM}{N}(12(P\frac{L_w}{N})^2 + 12P\frac{L_w}{N}) + \\ + \ (2M + P)C_{\text{bank}} \quad . \qquad (22)$$

Under the assumption of only moderate oversampling $K/N \approx 1$, for large L_w the cost of the subband version compared to its fullband counterparts in (19) is therefore reduced by a factor of N^2. Although the RLS algorithm imposes a greater computational load per iteration than the NLMS, it superior convergence — due to its independence of temporal and spatial correlations in the P input signals to the MISO RLS equalisers — may make a deployment desirable. Considering that the

number of required iterations for training may be much shorter than under the NLMS, the overall cost of a subband RLS MISO equaliser could be lower than with the NLMS.

5 SIMULATIONS

In the following we present a comparison of the various discussed algorithms. The environment in which these simulations are performed is characterised first.

5.1 MIMO Channel Model and Simulation Parameters

We use a Saleh-Valenzuela (SV) statistical indoor model to generate realistic channel impulse responses (CIRs) [16]. The SV model produces a clusters of rays according to an exponential distribution. Following the suggestions in, we have simulated CIRs at a sampling rate of 100MHz with a mean cluster arrival time $1/\Lambda = 300$ ns, a mean ray arrival time $1/\lambda = 5$ ns, a cluster power decay time constant $\Gamma = 60$ ns and the ray power decay time constant $\gamma = 20$ ns [16]. We generate four of these channels independently to create a 2×2 broadband MIMO channel. Simulations are then run on an ensemble of such 2×2 MIMO channel realisations.

For the MIMO equaliser, we have selected a delay $\delta = L_w/2$ to address the non-minimum phase characteristic of the channel. For the NLMS adaptations we use $\tilde{\mu} = 0.18$ and for the RLS adaptation $\beta = 1$. For the fullband system we use $L_w = 280$, and for the equivalent subband system $K = 16$, $N = 14$ based on a prototype filter with $L_p = 448$ taps resulting in the characteristic given in Fig. 4 and have set $L_w/N = 20$ as filter length in the subband case.

5.2 Computational Complexity

The complexity of various systems is compared in Fig. 7 for the subband parameters stated in Sec. 5.1. In general, the subband approach can substantially reduce the computational complexity and would amount to 14.6% and 0.6% for $L_w = 280$ of their fullband equivalents for LMS and RLS, respectively.

5.3 Convergence

Fig. 8 shows the ensemble MSE of the various systems in a noiseless environment, whereby the fullband RLS has been omitted due to its large complexity. We see that the subband NLMS system converges faster than the fullband system due to the filter banks' whitening effect, but is considerably slower than the RLS solution. Given the analysis in Sec. 5.2, a subband RLS with its drastically reduced complexity compared a fullband version may be in reach for implementation, and about an order of magnitude more costly than a subband NLMS in terms of complexity.

5.4 BER Performance

Figure 9 shows the SNR versus BER performance for the systems considered uses BPSK under additive white Gaussian noise (AWGN) conditions, in addition to the curve for the optimum MMSE equaliser calculated using the analytic method outlined in Sec. 2.2 as a benchmark. For all noise levels and individual runs in the ensemble, the NLMS adaptations were terminated after 20,000 iterations and the RLS after 10,000 iterations. The bit error ratio (BER) was measured based on the adapted responses.

We see that the performance of the fullband and subband NLMS adapted equalisers are similar, with the subband equalisers performing slightly better at higher SNRs. This is due to the faster convergence of the subband NLMS as noted in Sec. 5.3, as the proposed subband MIMO equaliser converges faster, and the steady state has not necessarily been reached after the given permitted training interval. The RLS performance is superior in accordance with Fig. 8.

5.5 Discussion

The subband RLS cost per iteration is greater than that of the subband NLMS. However due to its much faster convergence, the RLS can be beneficial when the overall cost to reach a given MSE is considered. When operating in an environment with AWGN at 10dB SNR, the subband RLS adaptation can be terminated after approximately 1,000 iterations, resulting in a total of 8.1×10^6 MACs. The subband NLMS algorithm needs to be executed for about 25,000 iteration resulting in a cost of approximately 46.3×10^6 MACs to converge close to a similar MSE. In this respect, we have noted that the higher the SNR the greater the computational advantage given by the subband RLS over the subband NLMS will be. In fact, the subband NLMS will result in fewer computations only for very lower SNR (less than about 3.5 dB for the above simulations), as the noise floor and therefore the steady state performance is reached quickly. Also note that if the system operates in a non-stationary environment and the adaptive MIMO equaliser needs to track any channel changes, the RLS can be inferior to the NLMS' performance [15].

6 CONCLUSIONS

A subband adaptive MIMO equaliser structure has been presented. We have demonstrated that for highly time-dispersive MIMO channels, subband NLMS MIMO equaliser can benefit from spectral whitening through the subband decomposition as compared fullband counterpart, while additionally a reduction in computational complexity by a factor of approximately N is gained. An even higher reduction of N^2 was found for the subband RLS MIMO equaliser.

In simulations, subband MIMO equalisers performed better than the NLMS fullband approach in term of con-

vergence speed and BER after a limited number of iterations. The RLS showed the fastest convergence and approached the MMSE solution closely.

REFERENCES

[1] G. J. Foschini and M. J. Gans, "On limits of wireless communications in a fading environment when using multiple antennas," *Wireless Personal Communcations*, , no. 6, pp. 315–335, 1998.

[2] P. A. Nelson, H. Hamada, and S. J. Elliot, "Adaptive Inverse Filters for Stereophonic Sound Reproduction," *IEEE Transactions on Signal Processing*, vol. 40, no. 7, pp. 1621–1632, July 1992.

[3] O. Kirkeby, P. A. Nelson, H. Hamada, and F. Orduna-Bustamante, "Fast Deconvolution of Multichannel Systems Using Regularization," *IEEE Transactions on Speech and Audio Processing*, vol. 6, no. 2, pp. 189–194, March 1998.

[4] O. Kirkeby, P. A. Nelson, F. Orduna-Bustamante, and H. Hamada, "Local sound field reproduction using digital signal processing," *Journal of the Acoustical Society of America*, vol. Vol.100, no. No.3, pp. 1584–1593, March 1996.

[5] J. Benesty and D.R. Morgan, "Frequency-Domain Adaptive Filtering Revisited, Generalization to the Multi-channel Case, and Applications to Acoustic Echo Cancellation," in *Proc. IEEE International Conference on Acoustics, Speech and Signal Processing*, June 2000, vol. 2, pp. 789–792.

[6] W. Kellermann and H. Buchner, "Wideband Algorithms Versus Narrowband Algorithms for Adaptive Filtering in the DFT Domain," in *Proc. Asilomar Conference on Signals, Systems, and Computers*, November 2003.

[7] H. Yamada, H. Wang, and F. Itakura, "Recovering of Broadband Reverberant Speech Signal by Subband MINT Method," in *Proc. IEEE International Conference on Acoustics, Speech and Signal Processing*, April 1991, vol. 2, pp. 969–972.

[8] S. Weiss, G. W. Rice, and R. W. Stewart, "Multichannel equalization in subbands," in *Proc. IEEE Workshop on Applications of Signal Processing to Audio and Acoustics*, New Paltz, NY, October 1999, pp. 203–206.

[9] M. Miyoshi and Y. Kaneda, "Inverse Filtering of Room Acoustics", *IEEE Transactions on Acoustics, Speech and Signal Processing*, vol. 36, no. 2, pp. 145–151, Feb. 1988.

[10] V. Bale, *Computationally Efficient Equalisation of Broadband Multiple-Input Multiple-Output Systems*, Mini-Thesis, University of Southampton, UK, 2004.

[11] V. Bale and S. Weiss, "Comparison of Analytic Inversion Techniques for Equalisation of Highly Frequency-Selective MIMO Systems," in *Proceedings of Workshop on Signal Processing for Wireless Communications*, King College, London, UK, June 2004, pp. 150–155.

[12] S. Weiss and R. W. Stewart, *On Adaptive Filtering in Oversampled Subbands*, Shaker Verlag, Aachen, Germany, 1998.

[13] P. P. Vaidyanathan, *Multirate Systems and Filter Banks*, Prentice Hall, Englewood Cliffs, 1993.

[14] S. Weiss, "Analysis and fast implementation of oversampled modulated filter banks," in *Mathematics in Signal Processing V*, J. G. McWhirter and I. K. Proudler, Eds., chapter 23, pp. 263–274. Oxford University Press, March 2002.

[15] N.J. Bershad and O.M. Macchi, "Comparison of LMS and RLS Algorithms for Tracking a Chirped Signal," in *Proc. IEEE International Conference on Acoustics, Speech and Signal Processing*, Glasgow, Scotland, May 1989, vol. 2, pp. 896–899.

[16] A. A. M. Saleh and R. A. Valenzuela, "A Statistical Model for Indoor Multipath Propagation," *IEEE Journal on Selected Areas of Communications*, vol. 5, no. 2, pp. 128–137, February 1987.

[17] R. E. Crochiere and L. R. Rabiner. *Multirate Digital Signal Processing.* Prentice Hall, Englewood Cliffs, NJ, 1983.

[18] A. Gilloire and M. Vetterli. Adaptive Filtering in Subbands with Critical Sampling: Analysis, Experiments and Applications to Acoustic Echo Cancelation. *IEEE Transactions on Signal Processing*, SP-40(8):1862–1875, August 1992.

[19] S. Haykin. *Adaptive Filter Theory.* Prentice Hall, Englewood Cliffs, 2nd edition, 1991.

[20] W. Kellermann. Analysis and Design of Multirate Systems for Cancellation of Acoustical Echoes. In *Proc. IEEE International Conference on Acoustics, Speech, and Signal Processing*, volume 5, pages 2570–2573, New York, 1988.

[21] M. Harteneck, S. Weiss, and R. W. Stewart. Design of Near Perfect Reconstruction Oversampled Filter Banks for Subband Adaptive Filters. *IEEE Transactions on Circuits & Systems II*, 46(8):1081–1086, August 1999.

[22] H. Mohamad. *Subband Adaptive Equalisation for Communication Transceivers.* PhD thesis, University of Southampton, Dec. 2003.

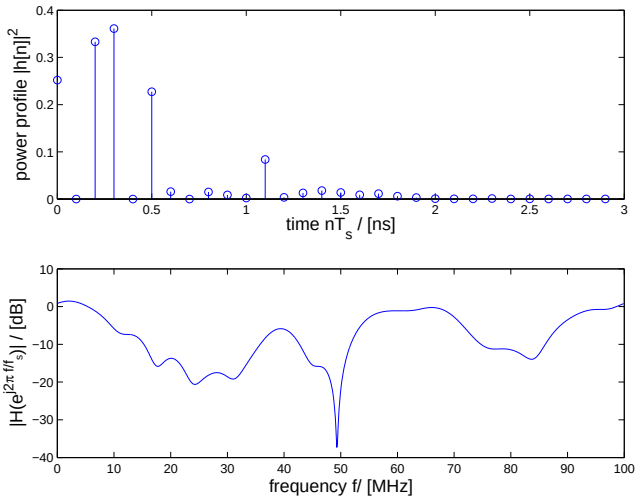

Figure 6: (top) CIR and (bottom) magnitude response of a sample channel generated by the SV model.

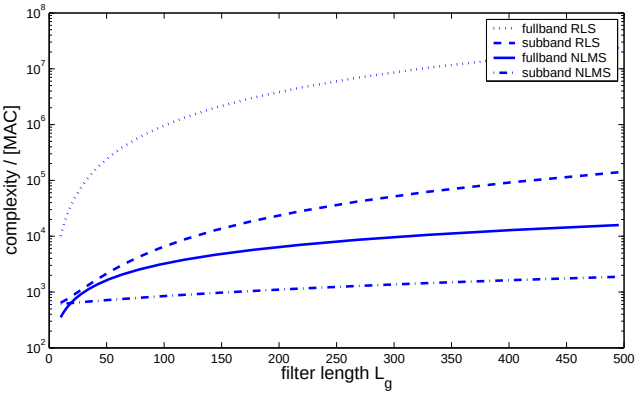

Figure 7: Computational complexities of NLMS and RLS implementations in both fullband and subband for $P = M = 2$; the subband system uses $K = 16$, $N = 14$, based on a prototype filter of length $L_{\mathrm{p}} = 448$.

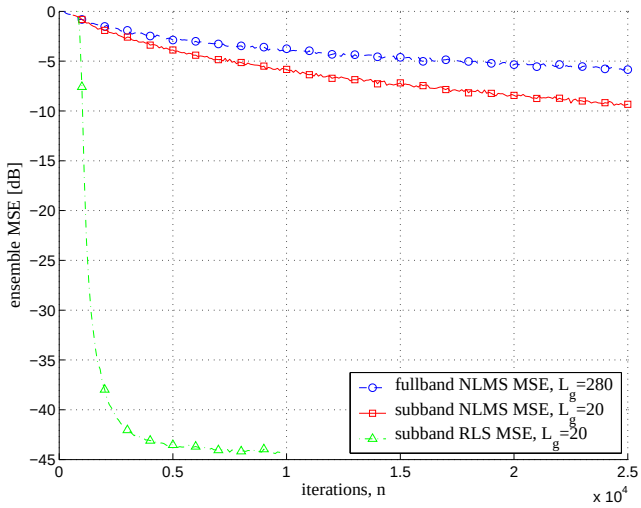

Figure 8: Subband and fullband NLMS and RLS ensemble MSE for a highly frequency-selective 2×2 MIMO channel.

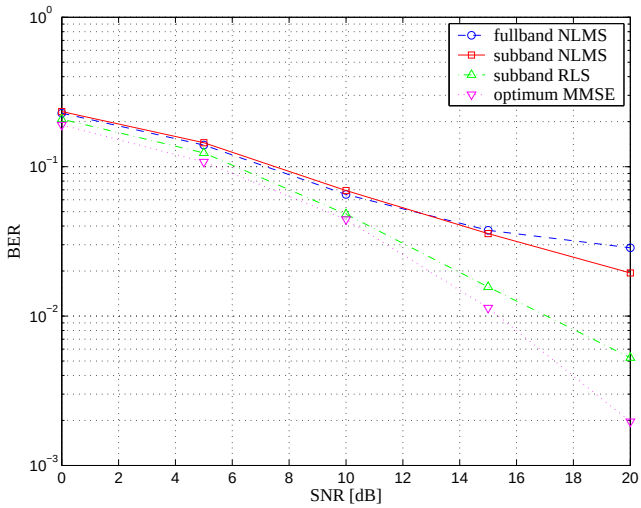

Figure 9: Subband and fullband NLMS and RLS SNR versus BER performance using BPSK for a highly frequency-selective 2×2 MIMO channel, and optimum MMSE performance for comparison.